
Numerical analysis of masonry structures by finite-discrete element model

Željana Nikolić*, Hrvoje Smoljanović and
Nikolina Živaljić

Faculty of Civil Engineering, Architecture and Geodesy,
University of Split,
Matice hrvatske 15,
Split 21000, Croatia
Email: zeljana.nikolic@gradst.hr
Email: hrvoje.smoljanovic@gradst.hr
Email: nikolina.zivaljic@gradst.hr
*Corresponding author

Abstract: This paper presents numerical model based on the finite-discrete element method for the analysis and prediction of the collapse of masonry structures with mortar joints and dry stone masonry structures. The model consists of a numerical model in a finite element, contact interaction algorithm which simulates the interaction between stone blocks in dry joint and numerical model in an interface element which simulates the behaviour of the mortar joints and unit-mortar interface. The verification of the model was performed on examples by comparing it with the known numerical and experimental results from literature.

Keywords: dry stone masonry structures; finite-discrete element method; masonry structures.

Reference to this paper should be made as follows: Nikolić, Ž., Smoljanović, H. and Živaljić, N. (2016) 'Numerical analysis of masonry structures by finite-discrete element model', *Int. J. Masonry Research and Innovation*, Vol. 1, No. 4, pp.330–350.

Biographical notes: Željana Nikolić, Position: full professor in structural mechanics, computational mechanics and earthquake engineering at University of Split, Faculty of Civil Engineering, Architecture and Geodesy; Head of the Department of Theory of Structures; Head of Master study, 'Modelling of the Structures'; Education: 1999, PhD, University of Split, Faculty of Civil Engineering; 1993, MSc, University of Split, Faculty of Civil Engineering, 1986 graduated in Civil Engineering, University of Split, Faculty of Civil Engineering; Awards: 1985 and 1986, Rector's awards, University of Split; 1986, Award for the best diploma work, Hidrotehnicki Institut 'Jaroslav Černi' Belgrade; Research activities: principal investigator and researcher at the projects funded by Croatian Science Foundation, Croatian Ministry of Science, Education and Sports and British-Croatian bilateral projects; Scientific papers: international journals 26, international conferences 45, domestic conferences 23, invited lectures 7, abstracts 19; Supervision of the students: graduate students 15, master students 1, doctoral students 4.

Hrvoje Smoljanović, citizenship: Croatian, occupation: Assistant Professor at the University of Split, Faculty of Civil Engineering, Architecture and Geodesy, Department for Theory of Structures, Split, Croatia; education: PhD in technical sciences, University of Split, Faculty of Civil Engineering, Architecture and Geodesy, 2013; graduated in Civil Engineering, University of Split, Faculty of Civil Engineering and Architecture Honours, 2005; also between 2002 and 2005 received Croatian Ministry of Science Scholarship for the years 2002, 2003, 2004 and 2005 and Rector's award and Dean's award for the following projects: Nonlinear dynamic analysis of three-dimensional reinforced concrete structures, scientific project funded by Croatian Ministry of Science, Education and Sport, Zagreb, Croatia 083-0831541-1532, PI prof. dr. sc. Željana Nikolić, 2007–2013.

Nikolina Živaljić, citizenship: Croatian, position: Assistant Professor at the University of Split, Faculty of Civil Engineering, Architecture and Geodesy, Department for Theory of Structures, Split, Croatia; education: PhD in Technical Sciences, University of Split, Faculty of Civil Engineering, Architecture and Geodesy, 2012; Master, University of Split, Faculty of Civil Engineering and Architecture, 2006; graduated in Civil Engineering, University of Zagreb, Faculty of Civil Engineering Training, 2000; Guest Researcher on the Queen Mary, University of London, 15 days, 2010; honours: 1998–2000 Croatian Ministry of Science, Education and Sports Scholarship; projects: Nonlinear dynamic analysis of three-dimensional reinforced concrete structures, scientific project funded by Croatian Ministry of Science, Education and Sport, Zagreb, Croatia 083-0831541-1532, PI prof. dr. sc. Željana Nikolić, 2007–2013; Nonlinear stability and bearing capacity of line and plate structures, scientific project financed by Croatian Ministry of Science, 0083051, PI prof. dr. sc. Ante Mihanović, 2002–2005.

This paper is a revised and expanded version of a paper entitled 'Numerical Analysis of Masonry Structures by Finite Discrete Element Model', presented at 29 September–02 October 2015, Opatija, Croatia.

1 Introduction

Building construction using dry stone walls or clay bricks which are held together by mortar is one of the oldest building techniques which are still in use today. Masonry has a long worldwide tradition of usage in construction due to its simplicity. In spite of the simplicity that is manifested during the construction of masonry structures, understanding and describing mechanical behaviour of those structures represents a true challenge due to the nature of masonry structure which shows a complex and particular nonlinear behaviour.

Most of the models for simulation of the behaviour of masonry structures are based on the finite element method. The analysis of masonry by finite element method is usually based on the modelling of the material as a fictitious homogeneous orthotropic continuum. Strong discontinuities between different units of the masonry can be simulated by joint interface elements (Calderini and Lagomarsino, 2008; Lourenço and Rots, 1997).

Another approach for modelling of the cracking in these materials is the discrete element method (Cundall and Hart, 1992; DeJong, 2009; Lemos, 1998; Baggio and

Trovalusci, 1995). The behaviour of masonry is based on the idealisation of the material as a discontinuum where joints are modelled as contact surfaces between different units. Different approaches in modelling of the contact exist. One of them is distinct elements method (Cundall and Hart, 1992) used at first to model rocky aggregates, then walls and granular materials, in software such as UDEC, TRIDEC. The second one is the non-smooth contact dynamics (NSCD) method, which has been initiated and developed by Jean and Moreau (1992; Jean, 1999) and applied in numerical simulation of monuments made of blocks (Acary and Jean, 1998). In NSCD, the basic laws such as Coulomb's law and the inelastic shock law are described as non-smooth laws and the dynamical equation is discretised according to a low-order implicit algorithm, while smooth approximations of these laws are used in distinct element method, together with an explicit scheme. Consequently, NSCD uses large time steps and needs many iterations at each time step, while distinct element method uses many small time steps and few iterations at each time step.

In recent times an increasing number of models attempted to combine the advantages of finite element and discrete element methods. The most often used numerical methods which combine these methods are discontinuous deformation analysis (Pearce et al., 2000) and combined finite-discrete element method (FEM/DEM) (Munjiza, Andrews and White, 1999). These methods are designed to handle contact situations in which transition from continua to discontinua can appear.

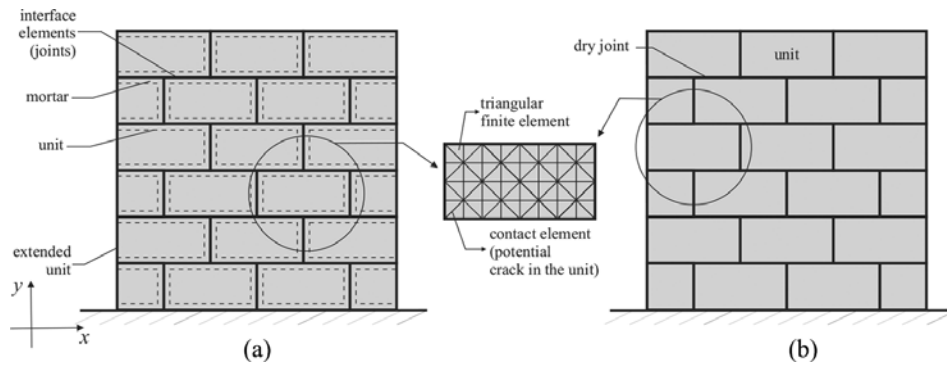
The FEM/DEM, the subject of this paper, was first developed for the simulation of fracturing problems considering deformable particles that may split and separate during the analysis. Within the framework of this method the discrete elements are discretised by constant strain triangular finite elements. Material nonlinearity, including fracture and fragmentation of discrete elements, is considered through contact elements (Munjiza, Andrews and White, 1999), which are implemented within a finite element mesh. The interaction between discrete elements is considered through the contact interaction algorithm based on the principle of potential contact forces (Munjiza and Andrews, 2000) and the Coulomb-type law for friction (Xiang et al., 2009). The method uses an explicit numerical integration of the equation of motion.

This paper presents numerical model based on FEM/DEM which can capture the main features related to the behaviour of dry stone masonry structure and masonry structures with mortar joints. The model consists of a numerical model in a finite element which simulates the behaviour of units, contact interaction algorithm for modelling of the interaction between stone blocks in dry joint and material model in an interface element which simulates the behaviour of the mortar joints and unit-mortar interface (Smoljanović, Živaljić and Nikolić, 2013; Smoljanović, 2013; Smoljanović, Nikolić and Živaljić, 2015).

The application of the model was performed on examples by comparing it with known numerical and experimental results from the literature.

2 Numerical model

In this numerical model masonry structure is considered as an assemblage of discrete elements as shown in Figure 1.

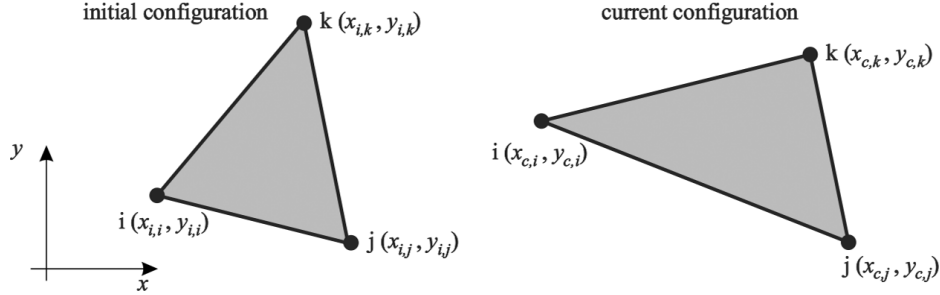
Figure 1 Discretisation of masonry structure: (a) mortar masonry; (b) dry stone masonry

Each discrete element, which can split and separate during the analysis, is discretised by its own mesh of constant strain triangular finite elements. Material behaviour in the finite elements is linear-elastic. Material nonlinearity, fracture and fragmentation are considered through the contact elements which are implemented within the finite element mesh of each block. The main processes included in the presented method are contact detection, contact interaction, finite strain elasticity as well as fracture and fragmentation, as explained in more detail later in this paper.

2.1 Deformability of finite elements

In the finite-discrete element framework, the deformability of discrete elements is enabled by means of a finite element mesh. Given the need for an algorithm that would be as simple and fast as possible and the fact that the calculation of contact forces is based on the same discretisation scheme, geometrically simple finite elements have been chosen for addressing linear problems, namely triangular, three-node finite elements with constant strain. However, by adopting constant strain triangular finite elements, shear members can become dominant in the stiffness matrix, causing an unrealistic increase in structure stiffness known as shear locking (Dow, 1999). The geometry of a triangular, three-node finite element is defined by global coordinates of each node (x, y) , where (x_i, y_i) represent the coordinates in their initial configuration and (x_c, y_c) are the coordinates in their current configuration (Figure 2). Since discrete elements are able to change their position in space, their displacements can be divided into two different components: displacements of discrete elements as rigid bodies caused by translation and rotation, and displacements resulting from the deformation of the body. Displacements of a deformable body involving rotation and deformation in the vicinity of a certain point of a deformable body are defined by the deformation gradient \mathbf{F} (Munjiza, 2004).

Figure 2 Initial and current configuration of a triangular finite element



The deformation gradient for three-node finite elements is constant in all points of the triangle and it can be obtained as follows:

$$\mathbf{F} = \begin{bmatrix} x_{c,j} - x_{c,i} & x_{c,k} - x_{c,i} \\ y_{c,j} - y_{c,i} & y_{c,k} - y_{c,i} \end{bmatrix} \begin{bmatrix} x_{i,j} - x_{i,i} & x_{i,k} - x_{i,i} \\ y_{i,k} - y_{i,i} & y_{i,k} - y_{i,i} \end{bmatrix}^{-1} \quad (1)$$

The Green-St Venant strain tensor \mathbf{E} is calculated from the following expression:

$$\tilde{\mathbf{E}} = \frac{1}{2}(\mathbf{F}\mathbf{F}^T - \mathbf{I}) \quad (2)$$

Adopting the linear-elastic relationship between the stress and strain, the Cauchy stress tensor can be obtained according the expression

$$\mathbf{T} = 2\mu\tilde{\mathbf{E}} + \lambda\varepsilon_v\mathbf{I} + \bar{\mu}\mathbf{D} \quad (3)$$

where μ and λ are the Lamé constants and ε_v is the volume deformation which is expressed by the following equation:

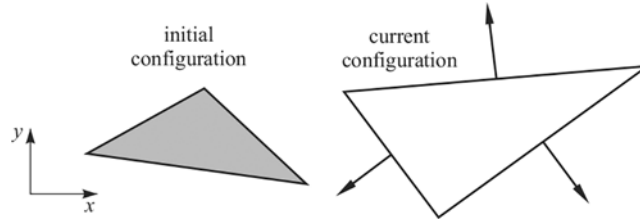
$$\varepsilon_v = \varepsilon_{xx} + \varepsilon_{yy} \quad (4)$$

The last element on the right-hand side of Eq. (3) represents the contribution of the deformation velocity where $\bar{\mu}$ is the damping coefficient and \mathbf{D} is the rate of the deformation tensor.

Traction force over each edge of the triangle can be calculated using the normal on the edge of the deformed configuration, with components of the normal given in the global frame (Figure 3). Edge traction is given by the expression

$$\mathbf{s} = \mathbf{T}\mathbf{n} = \begin{bmatrix} s_x \\ s_y \end{bmatrix} = \begin{bmatrix} t_{xx} & t_{xy} \\ t_{yx} & t_{yy} \end{bmatrix} \begin{bmatrix} n_x \\ n_y \end{bmatrix} \quad (5)$$

Figure 3 Normal vectors used in calculation of traction forces; magnitude of each normal is equal to the length of the corresponding edge



where n_x and n_y represent the components of the outward unit vector normal to the edges of triangle. Edge traction for each of the three edges of the deformed configuration is distributed proportionally to each of the nodes belonging to a particular edge. Equivalent nodal force in each node is represented by following expression:

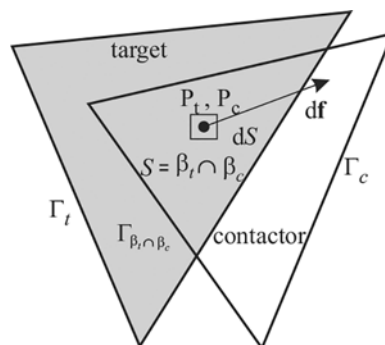
$$\mathbf{f} = \frac{1}{2} \mathbf{s} = \frac{1}{2} \begin{bmatrix} s_x \\ s_y \end{bmatrix} = \frac{1}{2} \begin{bmatrix} t_{xx} & t_{xy} \\ t_{yx} & t_{yy} \end{bmatrix} \begin{bmatrix} n_x \\ n_y \end{bmatrix} \quad (6)$$

2.2 Contact detection and interaction

The objective of the contact detection algorithm is to locate pairs of neighbouring finite elements that are in contact and to eliminate those that are too far away from one another and can no longer establish contact. Accordingly, the non-binary search algorithm for contact detection has been implemented into the FEM/DEM model (Munjiza, Andrews and White, 1998). The total time required for the detection of all contact pairs is proportional to the total number of discrete elements.

Once the pairs of discrete elements are detected, the algorithm of contact interaction (Munjiza and Andrews, 2000) defines the contact forces between two discrete elements, one of which is then designated as a contactor and the other as a target (Figure 4). In the interaction algorithm, the distributed contact forces are defined by the penalty method, which is based on the principle of potential contact forces. The contactor and the target overlap across the surface S bounded by the external edge $\Gamma_{\beta_t \cap \beta_c}$.

Figure 4 Contact force due to an infinitesimal overlap around points P_t and P_c



In such case, the total contact differential force on the contactor $d\mathbf{f}_c$ is defined as

$$d\mathbf{f}_c = p_0 [\text{grad}\phi_c(P_t) - \text{grad}\phi_t(P_c)] dS \quad (7)$$

where P_t and P_c are the points in which the target and the contactor overlap, ϕ is a corresponding potential function while p_0 is the penalty coefficient for normal contact forces (Munjiza, 2004). The total contact force is obtained by the integration of Eq. (7) across the entire overlapping surface S as follows:

$$\mathbf{f}_c = \int_{S=\beta_t \cap \beta_c} p_0 [\text{grad}\phi_c - \text{grad}\phi_t] dS \quad (8)$$

Equation (8) can be rewritten as

$$\mathbf{f}_c = p_0 \int_{\Gamma_{\beta_t \cap \beta_c}} \mathbf{n}_\Gamma [\phi_c - \phi_t] d\Gamma \quad (9)$$

where \mathbf{n}_Γ is the unit external normal on the edge Γ of the overlapping surface S .

In the framework of the contact forces algorithm, the Coulomb dry friction model for shear forces has been implemented as follows:

$$\mathbf{f}_t = -k_t \delta_t \quad (10)$$

where \mathbf{f}_t is the tangential elastic contact force, k_t is the penalty coefficient for friction and δ_t is the accumulated tangential displacement between two elements from the total previous history of the contact (Xiang et al., 2009).

If \mathbf{f}_t is greater than the maximum friction force defined by the Coulomb law $|\mathbf{f}_t| > \mu |\mathbf{f}_n|$, the elements slide along one another and the shear force between them is defined by means of the elastic normal force \mathbf{f}_n , according to the following expression:

$$\mathbf{f}_t = -\mu \mathbf{f}_n \quad (11)$$

where μ is the friction coefficient. In that case tangential displacement is equal to

$$\delta_t = -\frac{\mathbf{f}_t}{k_t} \quad (12)$$

2.3 Time integration of equation of motion

In the combined FEM/DEM, the shape and position of each discrete element is described by the current coordinates of finite elements nodes. To calculate the current coordinates of nodes, it is necessary to take into account the mass of the corresponding system. In the combined FEM/DEM, the mass of a system is concentrated in finite elements nodes, which leads to a lumped-mass model.

Time integration of the equations of motion for each corresponding node has been conducted explicitly using the finite differences method (Munjiza, 2004; Pearce et al., 2000), which is conditionally stable and whose stability and accuracy depend on the choice of a time step. The description of the update of variables can be written as

$$\begin{aligned} \mathbf{v}_{i,t+\Delta t/2} &= \mathbf{v}_{i,t-\Delta t/2} + \Delta t \mathbf{f}_{i,t} / m_i \\ \mathbf{x}_{i,t+\Delta t} &= \mathbf{x}_{i,t} + \Delta t \mathbf{v}_{i,t+\Delta t/2} \end{aligned} \tag{13}$$

where \mathbf{x}_i , \mathbf{v}_i , \mathbf{f}_i , m_i are the displacement vector, the velocity vector, the total mass vector and the mass of each node, respectively, and Δt is a time step. In this method, the time step significantly influences the numerical stability; namely, the central difference time integration scheme was applied. It is always numerically stable if the time step satisfies following expression

$$\Delta t \leq \frac{2}{\omega} \tag{14}$$

where ω is the highest frequency of the corresponding system. The conditions for the selection of time step are provided in Munjiza (2004). In addition, the time step depends on the penalty parameter. Increase of penalty parameter produces more accurate solutions but, due to the numerical stability, it causes smaller time steps (Munjiza, 2004).

2.4 Fracture and fragmentation

Fracture and fragmentation are essential processes in transition from continua to discontinua. In this numerical model it is realised by the combined single- and smeared-crack model, which is also known as the discrete-crack model.

In such a model, a typical stress-strain curve in direct tension is divided into two sections (Figure 5): strain-hardening prior to reaching the peak stress (f_t), which is easily implemented through the constitutive law, and strain-softening, for which the stress decreases with an increasing separation δ . It is modelled through a single-crack model (Figure 6) in contact elements implemented between finite element mesh.

Figure 5 (a) Strain-hardening and strain-softening curves defined in terms of strains and (b) strain-softening curve defined in terms of displacements

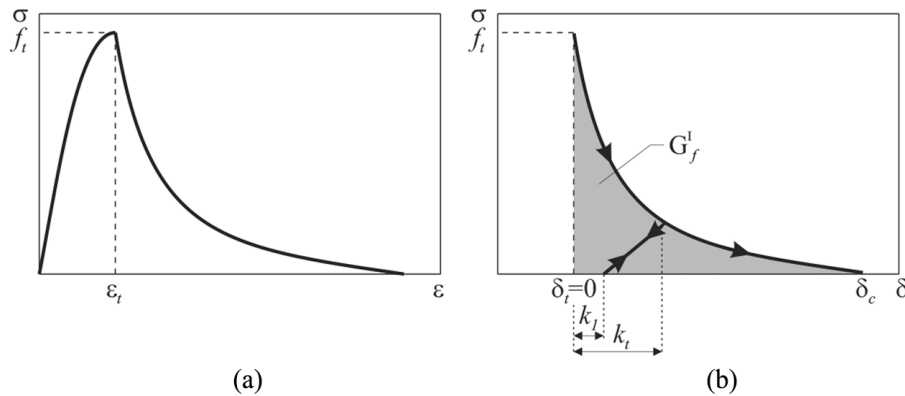
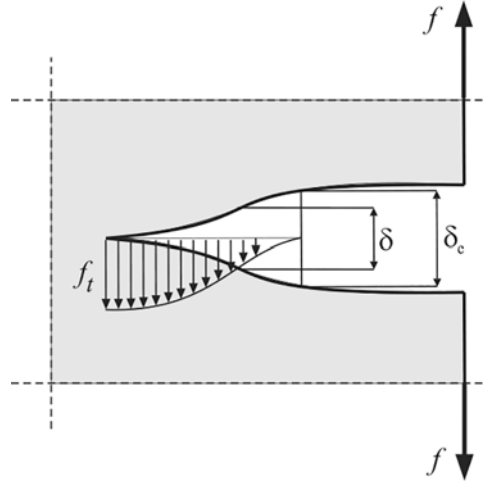


Figure 6 Single-crack model for the softening part of the stress-strain diagram

Source: Munjiza, Andrews and White, 1999

The cracks are assumed to coincide with the finite element edges (contact elements) which are achieved in advance through the topology of adjacent elements being described by different nodes. Separation of these edges induces a bonding stress which is taken to be a function of the size of separation δ (Figure 5). The area under the stress-displacement curve represents the energy release rate $G_f' = 2\gamma$, where γ is the surface energy, that is, the energy needed to extend the crack surface by a unit area (Munjiza and Andrews, 2000). In theory no separation occurs before the tensile strength f_t is reached, that is, $\delta = \delta_t = 0$, where δ_t is normal displacement at interface and contact element corresponding to tensile strength. In the actual implementation, it is enforced through the penalty function method (Munjiza and Andrews, 2000).

After reaching tensile strength f_t , stress decreases with an increasing separation δ while the bonding stress tends to be zero for critical separation $\delta = \delta_c$. For the separation $\delta_t < \delta < \delta_c$, the bonding stress is given by

$$\sigma = z f_t \quad (15)$$

where z is a heuristic scaling function representing an approximation of the experimental stress-displacement curves taken according to Smoljanović, Živaljić and Nikolić (2013)

$$z = \left[1 + (c_1 D_t)^3 \right] e^{-c_2 D_t} - D_t (1 + c_1^3) e^{-c_2} \quad (16)$$

where $c_1 = 3$ and $c_2 = 6.93$, while the damage parameter D_t is determined according to the following expression:

$$D_t = \begin{cases} (\delta - \delta_t) / (\delta_c - \delta_t), & \text{if } \delta_t < \delta < \delta_c; \\ 1, & \text{if } \delta > \delta_c \end{cases} \quad (17)$$

In this paper the numerical model in the contact element is extended to capture the main features related to cyclic behaviour as shown in Figure 5b, where the value k_1/k_t is equal to 0.73 as recommended by Reinhardt (1984).

The edges of two adjacent elements are held together by the shear stress calculated by the penalty function method (Munjiza and Andrews, 2000). After reaching shear strength f_s , which coincides with sliding $t = t_s$, the stress decreases with an increasing sliding t according to the exponential law defined by Eq. (16). At $t = t_c$ shear stress tends to be zero. For sliding $t_s < |t| < t_c$ shear stress is given by

$$\tau_c = z.f_s \quad (18)$$

where z is a heuristic scaling function given by Eq. (16) in which the damage parameter D_1 is replaced with shear damage parameter D_s given by

$$D_s = \begin{cases} (t-t_s)/(t_c-t_s), & \text{if } t_s < t < t_c; \\ 1, & \text{if } t > t_c \end{cases} \quad (19)$$

Within the framework of the FEM/DEM method the masonry structure is considered as an assemblage of extended unit elements connected with zero-thickness interface elements (Figure 1) which simulate the behaviour of the mortar joints and unit-mortar interface.

The dimensions of each unit are extended to the axis of the horizontal and vertical joints. Each unit element is discretised with its own constant strain triangular finite element mesh.

In this paper the existing FEM/DEM model is extended by a new material model in finite elements which takes into account the orthotropic behaviour of masonry, whose principal material axes coincide with the global axes x and y . It is known that, under uniaxial compressive loading, mortar tends to expand laterally more than the brick because of its weaker mechanical properties. Due to the continuity between bricks and mortar, ensured by cohesion and friction, mortar is confined laterally by the bricks. Thus, shear stress, developed at the mortar-brick interface, produces a triaxial compressive stress state in the mortar and bilateral horizontal tension coupled with vertical compression in the brick. In this way, failure usually occurs by the development of cracks in the bricks, parallel to the loading direction. This effect of softening and failure in compression is taken into account in finite element. Potential cracks in units due to tension and shear are considered through contact elements, implemented between the finite element mesh, and are based on a combined a single- and a smeared-crack model (Munjiza, Andrews and White, 1999) previously presented.

In this paper the new material model in an interface element which simulates the behaviour of the mortar joints and unit-mortar interface was also presented. The model takes into account the tension and shear strength (cohesion) of the mortar increasing the fracture energy in shear due to increasing pre-compression stress, decreasing friction coefficient due to increasing shear displacement and the cyclic behaviour in the interface element.

This new numerical model of the interface element and the new material model in a finite element, which were developed as part of this study, are shown below.

2.5 Numerical model in finite element

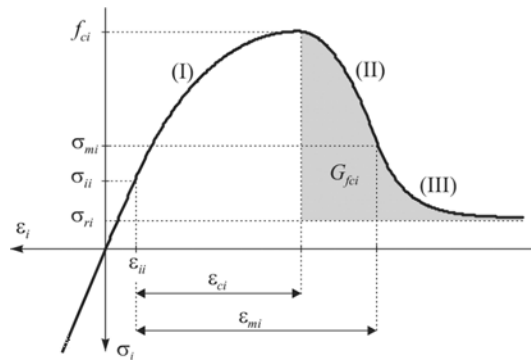
Due to the geometrical arrangement of units and mortar, the constitutive behaviour of masonry is highly anisotropic, even if the properties of these constituents are isotropic. Oriented voids in perforated unit elements also contribute to the anisotropic behaviour of

masonry structures whose material axis, in most cases, coincides with horizontal and vertical directions.

Unlike concrete structures in which the collapse usually appears due to cracking of material in tension or shear, in masonry structures, besides these two failure mechanisms, the material often crushes in compression. This failure mechanism may be especially important in masonry structures built with perforated bricks.

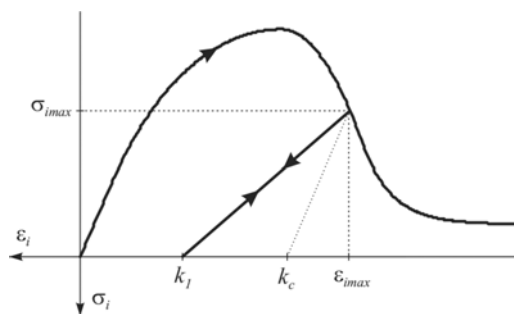
In this paper, the orthotropic constitutive material behaviour with hardening/softening law for compression is considered in finite elements (Lourenço, 1996; Smoljanović, Nikolić and Živaljić, 2015). Elliptical hardening followed by parabolic/exponential softening law in compression defined by four inelastic parameters - $(\sigma_p, \varepsilon_i)$, $(\sigma_m, \varepsilon_m)$, (f_c, ε_c) , $(\sigma_r, \varepsilon_r)$ - is shown in Figure 7 where the subscripts i , m , c and r denote, respectively, the initial, medium, compressive peak and residual values. This hardening/softening behaviour is considered for both material axes, with different compressive fracture energies and different compressive strengths. A redefined compressive fracture G_{fci} corresponds only to the local contribution of σ_i - ε_i diagram, where subscript i refers to the material axes which correspond to global axes x and y .

Figure 7 Hardening/softening law for compression



Cyclic behaviour is adopted as shown in Figure 8 where k_1 is plastic strain for zero stress after unloading from monotonic tensile envelope, while k_c is plastic strain for zero stress after unloading from monotonic tensile envelope according to initial modulus of elasticity. The ratio of k_1/k_c , adopted as 0.935, is obtained from numerical analyses (Smoljanović, 2013) to achieve the best correlation with experimental results.

Figure 8 Cyclic behaviour in compression



2.6 Numerical model in interface element

The numerical model in the interface element simulates the behaviour of the mortar joints and unit-mortar interface taking into account cracking of joints in tension and sliding along the bed or head joints in shear. Since the contact elements describe discontinuity in a displacement field after reaching ultimate tension or shear strength, their behaviour is described in terms of the relationship between stress and relative displacement based on a single- and smeared-crack model (Munjiza, Andrews and White, 1999). When relative displacement exceeds critical displacement, interface element disappears and contact interaction between fragmented parts is considered according to potential contact forces (Munjiza and Andrews, 2000), taking into account Coulomb's dry friction model (Xiang et al., 2009).

Since the experimental research conducted by Van der Pluijm (1993) has shown that increasing the pre-compression stress levels in the contact between the block and the mortar causes an increase in the fracture energy in shear, in the presented model, this phenomenon is taken into account according to the following relation

$$G_f'' = G_{f0}'' - C\sigma \quad (\text{N/m}) \quad (20)$$

where G_{f0}'' is the value of the shear fracture energy in the case when the normal pre-compression stress is equal to zero, C is constant in m and σ is pre-compression stress in MPa. In the presented numerical model, constant C is adopted as 106.31 m (Smoljanović, 2013), to obtain the best correlation with experimental results reported by Van der Pluijm (1993).

3 Numerical examples

3.1 Sensitivity study of penalty coefficient

Application of the penalty method in calculation of the contact forces in FEM/DEM influences solution accuracy. The errors arise due to the penetration of discrete elements into each other during the contact interaction or due to the separation of finite elements before the appearance of cracks, which is regulated with the value of penalty coefficient. The value of penalty coefficient p_0 could be chosen extremely high in order to eliminate errors, but this would lead to very small time step and very long calculation time. In numerical examples analysed by FEM/DEM it is recommended to choose minimal value of penalty coefficient, which would result in acceptable errors.

In this example, an analysis of the influence of the penalty coefficient on relative error was analysed. For this purpose, a dry stone masonry column consisting of 10 stone blocks and exposed to monotonic increasing vertical load at the top was analysed. This force causes the vertical displacement at the top of the column, which can be analytically determinate according to

$$\Delta h = \frac{Fh}{EA} \quad (21)$$

where F , h , E and A are the forces at the top of the column, column height, modulus of elasticity and cross-section area, respectively. Based on the known analytical solution and numerical results, relative error can be obtained.

Geometry and discretisation of the column used in numerical analysis are shown in Figure 9, while the adopted characteristics of the stone are shown in Table 1.

Figure 9 Dry stone masonry column: (a) geometry; (b) discretisation

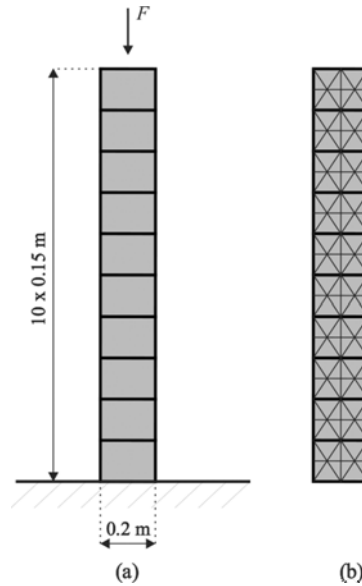


Table 1 Mechanical characteristics of stone used in numerical analysis

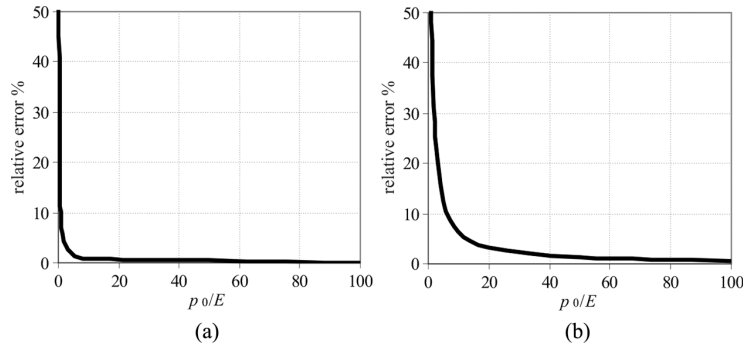
<i>Modulus of elasticity (MPa)</i>	<i>Poisson coefficient</i>
20000	0.0

The analysis was conducted with and without contact elements between triangular finite element mesh with various values of the penalty coefficient. In the case when there are no contact elements between triangular finite elements, the error in numerical solution gets erased due to the penetration of stone blocks into each other at dry contact. This penetration is regulated with penalty coefficient in contact interaction algorithm based on potential contact force. In the case when contact elements are implemented between finite elements mesh (fragmentation of each block is enabled), the error in numerical solution gets erased not only due to the penetration of stone blocks into each other at dry contact but also due to the penetration of triangular finite elements of corresponding stone blocks into each other.

Figure 10a and 10b show the value of the relative error of vertical displacement of the top of the column in cases with and without contact elements between finite elements depending on the value of penalty coefficient. It can be seen that in both cases the value of the relative error decreases with increasing penalty coefficient. In the case without contact elements, the value of the relative error is less than 1% if the value of penalty coefficient is 10 times greater than the modulus of elasticity of stone. In the case with

contact elements, the value of the relative error is less than 1% if the value of penalty coefficient is 100 times greater than the modulus of elasticity. A further increase in the value of penalty coefficient leads to further reduction of the relative error.

Figure 10 Relative error dependence on the value of penalty coefficient p_0 : (a) without contact elements (b) with contact elements

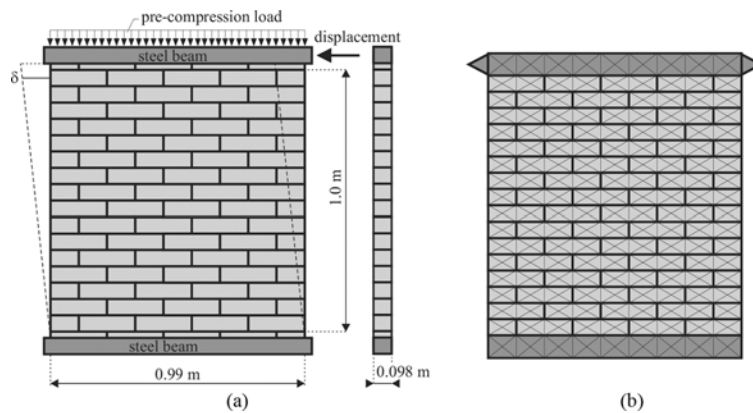


3.2 Masonry shear walls exposed to a monotonically increasing loading

In this example, the ability of the numerical model to reproduce the main features that characterise the behaviour of masonry shear walls under increasing monotonic increasing is performed by comparing experimental and numerical results. The numerical analyses were performed on several shear walls which Rajmakers and Vermeltoort (1992) analysed within the CUR (Council on Undergraduate Research) project. The walls analysed in this example correspond to the samples J4D, J5D and J7D.

Geometrical characteristics of the walls are shown in Figure 11. The walls have a width/height ratio of one with dimensions $990 \times 1000 \text{ mm}^2$ and consist of 18 rows of blocks, where only 16 between them were active, while the remaining two were clamped in the steel beams (Figure 11a). The walls were made of solid clay bricks with dimensions $210 \times 98 \times 50$ and 10-mm thick mortar. Discretisation of the structure with finite element mesh used in the numerical analysis is shown in Figure 11b.

Figure 11 Masonry shear wall: (a) geometry; (b) finite element mesh



Different vertical pre-compression stresses were applied to the walls (0.3 MPa for walls J4D and J5D and 2.12 MPa for wall J7D) keeping the bottom and top boundaries horizontal and precluding any vertical movement at the bottom of the wall. After applying the vertical stress, the walls were exposed to the horizontal load, which is achieved through the controlled displacement of steel beam at the top of the walls. The loading rate was 20 $\mu\text{m/s}$ in order to obtain quasi-static loading procedure. During the application of the horizontal displacement, vertical movements of the top and bottom of the steel beams were prevented.

Mechanical characteristics of materials used in numerical analysis are based on data taken from the literature (Raijmakers and Vermeltoort, 1992) and shown in Table 2. In this table index x refers to horizontal direction, while index y refers to vertical direction.

Table 2 Mechanical characteristics of materials

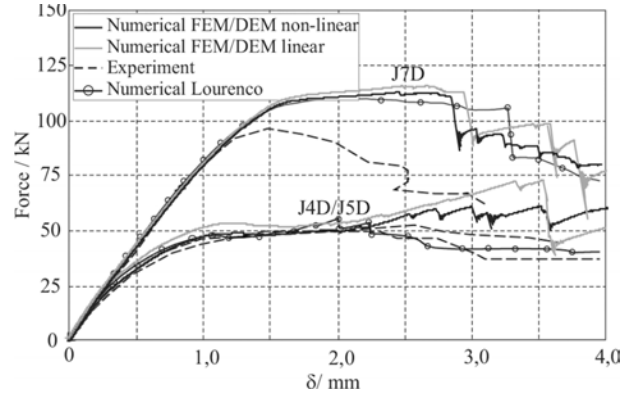
Unit				
Young modulus E_x/E_y (MPa)	Poisson ratio, ν_{xy}	Compressive strength, $f_{cx} = f_{cy}$ (MPa)	Tensile strength, f_t (MPa)	Shear strength, f_s (MPa)
7520/3960	0.09	10.5	2.0	2.8
Fracture energy in tension/shear, G_f^I / G_f^{II} (N/m)		Fracture energy in compression, G_{fcx} / G_{fcy} (N/m)	Friction coefficient initial/residual, μ_0/μ_r	
80/500		20000/15000	1.0/1.0	
Interface element				
Tensile strength, f_t (MPa)	Shear strength, f_s (MPa)	Fracture energy in tension/shear, G_f^I / G_f^{II} (N/m)	Friction coefficient initial/residual, μ_0/μ_r	
0.16	0.224	18/50	0.75	

In the performed analysis, the relationship between the horizontal displacement and the horizontal force at the top of the wall was measured. Numerical analyses were performed using both nonlinear material model and linear elastic numerical model of the finite element method as discussed earlier in this paper (Munjiza, 2004).

A comparison of numerical results obtained in this paper with the experimental results reported in Raijmakers and Vermeltoort (1992) and numerical results obtained by Lourenço (1996) are shown in Figure 12.

The numerical results of Lourenço were obtained by a numerical model based on the finite element method in which the units were discretised with continuum elements while the joints were discretised with interface elements. A composite interface model, which includes softening for tension, shear and compression, was based on the modern plasticity concept.

Figure 12 Comparison of experimental and numerical displacements at the top of the wall



Particularly for walls J4D and J5D, good agreement can be observed between the numerical results obtained in this study by the nonlinear model based on FEM/DEM and the experimental and numerical results obtained by Lourenço (1996).

In the case of wall J7D, the numerical results obtained by the nonlinear FEM/DEM model do not show a significant difference compared to the numerical results obtained by Lourenço (1996). On the other hand, all the numerical results provide approximately 15% higher ultimate load for wall J7D compared to those obtained by the experiment (Raijmakers and Vermeltoort, 1992). It can be also seen that the numerical results obtained with linear material model in the finite element method provide approximately 25% higher ultimate load for walls J4D/J5D compared to those obtained by the nonlinear numerical model. For wall J7D there is no significant difference between the numerical results obtained by linear and nonlinear models since the collapse appeared due to exceeding shear strength of the wall.

Failure patterns, just before the complete breakdown, obtained from experiments (walls J4D/J5D) and numerical analyses are compared and presented in Figure 13. It can be seen that experimental and numerical crack patterns are similar. At the early loading stage the horizontal tensile cracks developed at the bottom and top of the wall, but diagonal stepped crack with cracks in the units led to the collapse of the wall.

Figure 13 Crack pattern in walls: (a) this work; (b) wall J4D, experiment by Lourenço (1996); (c) wall J5D, experiment by Lourenço (1996)

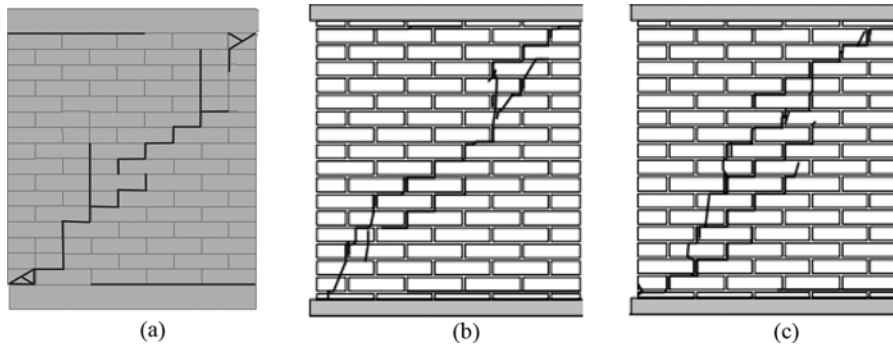
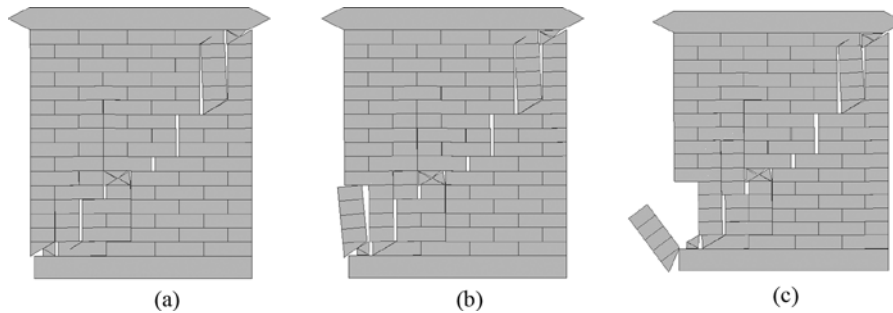


Figure 14 shows the behaviour of the wall after collapse. This example highlights the ability of a combined FEM/DEM in simulating the behaviour of the structure after reaching ultimate load, which can be important in analysing the progressive collapse of structure.

Figure 14 Collapse mechanism of the wall at displacement: (a) $\delta = 18$ mm, (b) $\delta = 21$ mm and (c) $\delta = 24$ mm



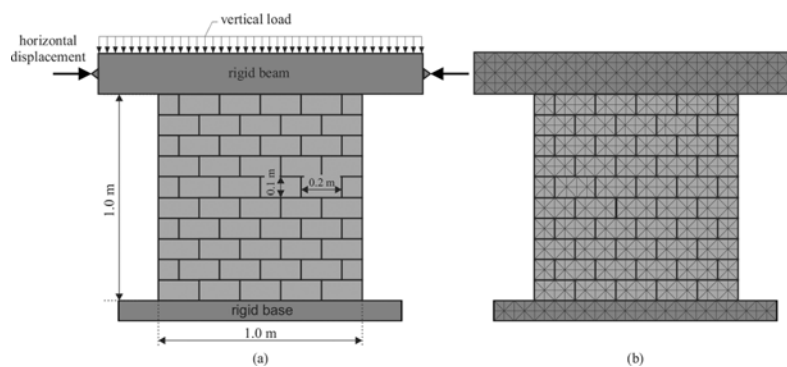
3.3 *Dry stone wall exposed to monotonically increasing loading*

This example demonstrates the ability of the numerical model to reproduce the main features that characterise the behaviour of dry stone masonry shear wall under monotonically increasing horizontal displacement.

For this purpose, the experimental program conducted by Oliveira (2003) was chosen to compare the experimental results with the numerical results obtained by FEM/DEM method.

The experimental program consisted of a series of quasi-static monotonic tests conducted on a small stone wall sample whose geometry is shown in Figure 15a. The wall discretisation used in numerical analysis is presented in Figure 15b.

Figure 15 Schematic view of a stone wall: (a) geometry and load; (b) discretisation of the structure



The wall consisted of stone blocks of regular dimensions. Average values of the mechanical characteristics of the granite used in the experiment are taken from literature and are presented in Table 3.

Table 3 Mechanical characteristics of stone used in numerical analysis

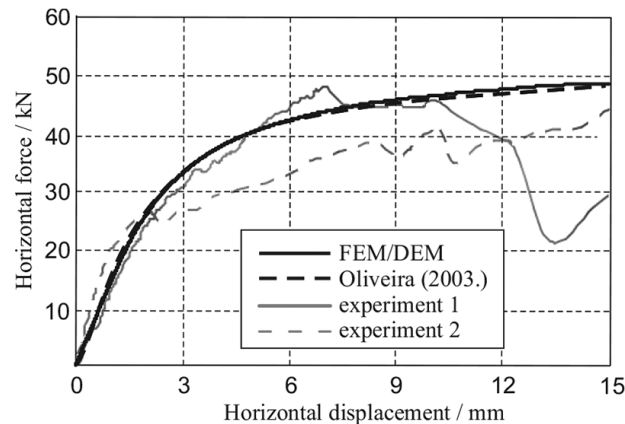
Modulus of elasticity (MPa)	Tensile strength (MPa)	Compressive strength (MPa)	Fracture energy (N/m)
15500	3.7	57.0	110

Source: Oliveira; 2003

The shear behaviour of walls was analysed for a vertical longitudinal force of 100 kN, which corresponds to the pre-compression stress of 0.5 MPa. The coefficient of friction $\mu = 0.62$ between stone blocks was obtained by experiment (Oliveira, 2003). After applying vertical stress, the wall was exposed to the horizontal load, which is achieved through the controlled displacement of the rigid beam at the top of the wall. The loading rate was 20 $\mu\text{m/s}$ in order to obtain quasi-static loading characteristics.

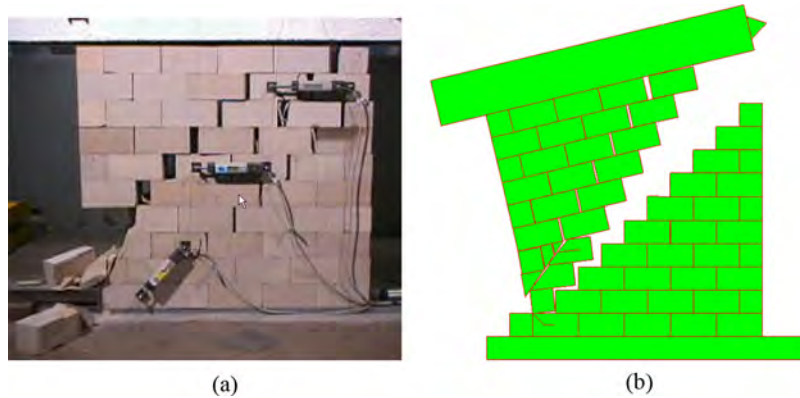
Comparison of experimental results (Oliveira, 2003), numerical results obtained by Oliveira (2003) and numerical results obtained by the presented numerical model is shown in Figure 16. The numerical model developed by Lourenco and Rots is based on the finite element method containing also contact elements whose constitutive law of behaviour is based on the theory of plasticity.

Figure 16 Comparison of numerical and experimental results



A good correspondence can be observed between results obtained by model based on the FEM/DEM method and numerical results obtained by Oliveira (2003). The correspondence between numerical and experimental results can be considered satisfactory taking into account the fact that the experiment was conducted with a dry wall made of natural stone. In such walls, the irregularities between blocks has a considerable effect on wall behaviour, and this effect is very hard to model by numerical procedure. The comparison of failure mode obtained by numerical model and physical experiment is presented in Figure 17. It can be observed that failure of wall appears by rotation of the wall accomplished by cracking of stone blocks, and the FEM/DEM model used in the study reproduced these effects accurately.

Figure 17 Failure mechanism of wall: (a) experimental; (b) numerical (see online version for colours)



4 Conclusion

This paper presents a numerical model for the analysis and prediction of the collapse of dry stone masonry structures and masonry structures with mortar joints. The presented numerical model is based on the FEM/DEM and considers the numerical model in finite element, which simulates the behaviour of units; contact interaction algorithm, which simulates the interaction between stone blocks in dry joint; and a material model in an interface element used for simulating the behaviour of the mortar joints and unit-mortar interface.

Material model in finite element takes into account orthotropic and cyclic behaviour, failure, and softening. The interaction between stone blocks in dry joint is considered through the contact interaction algorithm based on the principle of potential contact forces and the Coulomb-type law for friction, while the numerical model in contact element takes into account the possibility of failure and softening behaviour in tension and shear, increasing the fracture energy in shear due to increasing pre-compression stress, decreasing friction coefficient due to increasing shear displacement and the cyclic behaviour in interface element.

The performance of the presented numerical model was investigated using two masonry walls with mortar joints and one dry stone masonry shear wall. The numerical results show that the presented model is able to capture the main features that characterise the behaviour of masonry shear walls through the whole range of loading history.

The advantage of the presented model is its ability to simulate the behaviour of the masonry structure through the entire failure mechanism from the continuum to the discontinuum using the discrete representation of cracks and discontinuities.

Acknowledgements

This work has been fully supported by Croatian Science Foundation under the project ‘Development of Numerical Models for Reinforced-Concrete and Stone Masonry Structures under Seismic Loading Based on Discrete Cracks’ (IP-2014-09-2319).

References

- Acary, V. and Jean, M. (1998) Numerical simulation of monuments by the contact dynamics method. DGEMN-LNEC-JRC. Monument-98, Workshop on seismic performance of monuments, November 1998, Lisbon, Portugal, pp.69–78.
- Baggio, C. and Trovalusci, P. (1995) ‘Stone assemblies under in-plane actions-comparison between nonlinear discrete approaches’, *Computer Methods in Structural Masonry*, Vol. 3, pp.184–193.
- Calderin, C. and Lagomarsino, S. (2008) ‘Continuum model for in-plane anisotropic inelastic behaviour of masonry’, *Journal of Structural Engineering*, Vol. 134, No. 2, pp.209–220.
- Cundall, P.A. and Hart, R.D. (1992) ‘Numerical modelling of discontinua’, *Engineering Computations*, Vol. 9, pp.101–113.
- DeJong, M.J. (2009) *Seismic Assessment Strategies for Masonry Structures*, Dissertation, Massachusetts Institute of Technology, Massachusetts.
- Dow, J.O. (1999) *A Unified Approach to the Finite Element Method and Error Analysis Procedures*, Academic Press, San Diego.
- Jean, M. (1999) ‘The non smooth contact dynamics method’, in Martins, J.A.C. and Klarbring, A. (Eds.): *Computer Methods in Applied Mechanics and Engineering, Special Issue on Computational Modeling of Contact and Friction*, pp.235–257.
- Jean, M. and Moreau, J.J. (1992) ‘Unilaterality and dry friction in the dynamics of rigid bodies collections’, in Curnier, A. (Ed.): *Proc. of Contact Mech. Int. Symp.*, pp.31–48.
- Lemos, J.V. (1998) ‘Discrete element modelling of the seismic behaviour of stone masonry arches’, in Pande, G.N., Middleton, J. and Kralj, B. (Eds.): *Computer Methods in Structural Masonry*, E & FN Spon, London, pp.220–227.
- Lourenço, P.B. (1996) *Computational Strategies for Masonry Structures*, PhD Thesis, Delft University of Technology, Delft.
- Lourenço, P.B. and Rots, J.G. (1997) ‘A multi-surface interface model for the analysis of masonry structures’, *Journal of the Engineering Mechanics ASCE*, Vol. 123, pp.660–668.
- Munjiza, A. (2004) *The Combined Finite-discrete Element Method*, 1st ed., John Wiley & Sons, The Atrium, Southern Gate, Chichester, West Sussex, England.
- Munjiza, A. and Andrews, K.R.F. (2000) ‘Penalty function method for combined finite-discrete element system comprising large number of separate bodies’, *International Journal for Numerical Methods in Engineering*, Vol. 49, pp.1377–1396.
- Munjiza, A., Andrews, K.R.F. and White, J.K. (1998) ‘NBS contact detection algorithm for bodies of similar size’, *International Journal for Numerical Methods in Engineering*, Vol. 43, pp.131–149.
- Munjiza, A., Andrews, K.R.F. and White, J.K. (1999) ‘Combined single and smeared crack model in combined finite-discrete element method’, *International Journal for Numerical Methods in Engineering*, Vol. 44, pp.41–57.
- Oliveira, D.V. (2003) *Experimental and Numerical Analyses of Blocky Masonry Structures under Cyclic Loading*, PhD Thesis, University of Minho, Guimarães, Portugal.
- Pearce, C.J., Thavalingam, A., Liao, Z. and Bićanić, N. (2000) ‘Computational aspects of the discontinuous deformation analysis framework for modelling concrete fracture’, *Engineering Fracture Mechanics*, Vol. 65, pp.283–298.
- Raijmakers, T.M.J. and Vermeltfoort, A.T. (1992) *Deformation Controlled Tests in Masonry Shear Walls*, TNO-Bouw, Delft, Report No. B-92-1156.
- Reinhardt, H.V. (1984) ‘Fracture mechanics of an elastic softening material like concrete’, *Heron*, Vol. 29, No. 2, pp.3–41.
- Smoljanović, H. (2013) *Seismic Analysis of Masonry Structures with Finite Discrete Element Method*, PhD Thesis, University of Split, Split (in Croatian)

- Smoljanović, H., Nikolić, Ž. and Živaljić, N. (2015) 'A combined finite-discrete numerical model for analysis of masonry structures', *Engineering Fracture Mechanics*, Vol. 136, pp.1–14.
- Smoljanović, H., Živaljić, N. and Nikolić, Ž. (2013) 'A combined finite-discrete element analysis of dry stone masonry structures', *Engineering Structures*, Vol. 52, pp.89–100.
- Van der Pluijm, R. (1993) 'Shear behaviour of bed joints', in Hanid A.A. and Harris H.G. (Eds.): *North American Masonry Conference: Proceedings of the 6th North American Masonry Conference*, 1993, Philadelphia, Pennsylvania, USA, pp.125–36.
- Xiang, J., Munjiza, A., Latham, J.P. and Guises, R. (2009) 'On the validation of DEM and FEM/DEM models in 2D and 3D', *Engineering Computations*, Vol. 26, pp.673–687.